Levenspiel, O., D. Kunii, and T. Fitzgerald, "The Processing of Solids of Changing Size in Bubbling Fluidized Beds," *Power Technology*, **2**, 87 (1968/69).
Merrick, D., and J. Highley, "Particle Size Reduction and Elutriation in a Fluidized-Bed Process," *AIChE Symp. Ser.*, No. 137, **70**, 366 (1974).
Mori, S., and C. Y. Wen, "Estimation of Bubble Diameter in Gaseous Fluidized Beds," *AIChE J.*, **21**, 109 (1975).
Overturf, B. W., "PROPS: A Physical Properties Package for Computer Aided Design," Purdue Research Foundation, W. Lafayette, IN (1979).
Overturf, B. W., "Towards a Generalized Description of Gas-Solid Reaction in a Fluidized Bed Reactor," Ph.D. Thesis, Purdue University, W. Lafayette, IN (1980).
Overturf, B. W., and G. V. Reklaitis, "BED: A Generalized Model of a Fluidized Bed Gas-Solid Reactor," Purdue Research Foundation, W. Lafayette, IN (1980).
Overturf, B. W., and G. V. Reklaitis, "Fluidized Bed Reactors with Generalized Particle Balances. Part II: Coal Combustor Application," *AIChE J.*, **29**, (Sept., 1983).
Rajan, R., and C. Y. Wen, "Fluidized Bed Combustor Modelling," AIChE 86th National Meeting, Paper No. 57a, Houston (1979).
Shaw, I. D., T. W. Hoffman, and P. M. Reilly, "Experimental Evaluation of Two-Phase Models Describing Catalytic Fluidized Bed Reactors," *AIChE Symp. Ser.*, No. 141, **70**, 41 (1974).
Villadsen, J., and M. L. Michelson, *Solution of Differential Equation Models by Polynomial Approximation*, Prentice-Hall, Inc., Englewood Cliffs, NJ (1978).
Weimer, A. W., and D. E. Clough, "Dynamics of Particle Size/Conversion Distributions in Fluidized Beds: Application to Char Gasification," *Powder Tech.*, **26**, 11 (1980a).
Weimer, A. W., and D. E. Clough, "Modeling of Char Particle Size/Conversion Distributions in a Fluidized Bed Gasifier: Non-Isothermal Effects," *Powder Tech.* **27**, 85 (1980b).
Zenz, F. A., "Bubble Formation and Grid Design," *I. Chem. E. Symp. Ser.*, No. 30, London (1968).

Manuscript received October 6, 1981; revision received October 5, and accepted October 20, 1982.

Part II: Coal Combustion Application

The model described in Part I is applied to study an atmospheric fluidized-bed coal combustor. Extensive case studies are investigated on the effects of: enhanced grid region heat and mass transfer; bed void fraction; emulsion phase temperature; elutriation rates; reaction rate parameters; feed particle-size distribution; and particle superheat. Comparison is made with experimental results reported by Babcock and Wilcox. Proper representation of the grid region and use of actual feed distributions are shown to be essential to predicting combustor performance. Better particle elutriation and single-particle combustion submodels are found to be key requirements for improved combustor modeling.

B. W. OVERTURF
Tennessee Eastman Co.
Kingsport, TN 37660

and

G. V. REKLAITIS
School of Chemical Engineering
Purdue University
West Lafayette, IN 47907

SCOPE

Atmospheric fluidized-bed coal combustors (AFBC) have received considerable attention in recent years for use in commercial power generation and hence have also been subjected to extensive experimental and modeling studies. Typical operating conditions for such reactors are (Babcock and Wilcox, 1976): bed temperature, 760–1,100°C; particle size range, 150–2,500 μm; superficial gas velocity, 0.3–5 m/s; expanded bed height, 0.3 to 2m; and bed char fraction, 3 wt. %. The oxidizing medium for the bed is air and, as evident from the low-bed char fraction, the largest portion of the bed is noncombustible material: coal ash, limestone or dolomite. Important concerns in the utilization of AFBC's are the coal carbon losses which occur through elutriation and with bed solids withdrawal (Beer, 1976). Elutriation can, of course, be controlled by choosing larger particle sizes and lower gas velocities. However, small particles and large velocities favor higher particle combustion rates. Efficient design clearly requires a careful balance of these factors. A model which can accommodate polydispersed feeds and includes an adequate representation of the grid region can serve a very useful function in permitting studies of elutriation vs. combustion rate tradeoffs. Models reported in the literature do not incorporate these features. The model described in Part I does accomplish this and is applied in the present work to study the sensitivity of a simulated AFBC to key model parameters. Comparison is made to experimental results obtained by Babcock and Wilcox (1976) on a pilot unit.

CONCLUSIONS AND SIGNIFICANCE

On the basis of an extensive collection of simulation case studies, it can be demonstrated that the flue gas compositions as well as fixed carbon and oxygen conversions of an experimental fluidized-bed combustor can be predicted by suitable tuning of model parameters. More importantly, however, it is evident that

- Proper representation of the grid region is essential in combustor modeling. If, as is likely the case, most dilute to emulsion-phase transfer occurs in the grid region, bubbling-bed models may be of limited value in predicting reactor performance.
- Representation of reactive solids by an average size and density is adequate for the prediction of combustor performance. The key factor seems to be the sensitivity of particle elutriation rates to particle size (and density).
- Satisfactory modeling of combustors requires a more reliable prediction of single-particle elutriation rates and a more detailed description of single-particle combustion than is offered by the conventional single-film shrinking core model.

The overall reactor model used in this work forms a satisfactory tool for combustor studies and should remain useful when better elutriation and single-particle reaction submodels become available.

SINGLE-PARTICLE COMBUSTION

One of the four key components of any gas-solid fluid-bed model is the submodel which is used to represent the reaction of a single solid particle. In the present application, the reacting system consists of a char particle burning in an O_2-CO_2-N_2 environment. The key reactions which occur under conditions typical of char combustors are the heterogeneous reactions,

$$2C^* + O_2 \rightarrow CO \quad (1)$$

$$C^* + CO_2 \rightarrow 2CO \quad (2)$$

and the homogeneous reaction

$$2CO + O_2 \rightarrow 2CO_2 \quad (3)$$

where C* refers to the nonvolatile carbon present in the coal particle.

Since the rates of the heterogeneous reactions are generally fast, it is often assumed that these reactions can be lumped at the outer surface of the remaining carbon. Thus, a shrinking core particle reaction model is deemed to be appropriate. Much of the reaction modelling work has consequently focused on mass transfer and reaction in the boundary layer surrounding the particle. Several boundary layer models have been presented: The single-film model attributed to Nusselt, the two-film model proposed in 1931 by Burke and Shuman, and the simplified two-film model of Hougen et al. (1954) in which the heterogeneous rates were assumed to be diffusion-limited. As has been pointed out by Caram and Amundson (1977), the difference between the single- and two-film model lies in where the homogeneous CO oxidation reaction occurs: at the char surface, in the boundary layer, or in the bulk stream. Caram and Amundson (1977) presented computational results which verified that both the single- and two-film models were part of the general boundary layer solution. More recently Mon and Amundson (1978, 1979) used the Stefan-Maxwell equations and Schlichting's correlation to compute the molar flux in the boundary layer. This work shows that, first, for the low emulsion-phase O_2 concentrations typical of fluidized-bed combustors (about 5% O_2 or less) the single-film model should be valid over the entire range of particle sizes. Moreover, for sufficiently small particles, the single-film model should apply regardless of the bulk O_2 concentration. The very high (order of 1,000°C higher than the bulk gas temperature) particle temperature implied by the two-film model is contrary to experimental findings. Thus, it can be assumed that negligible CO oxidation will occur within the particle boundary layer. Secondly, for conditions typical of AFBC, the occurrence of a multiplicity of steady states for the single-particle balance equations is quite unlikely.

Having established that the homogeneous CO oxidation reaction occurs outside of the boundary layer, it remains to consider whether the heterogeneous reactions are kinetically or diffusionally limited. Field et al. (1967) present an expression for the C-O_2 reaction rate of the form:

$$r\left\{\frac{\text{mol carbon}}{\text{m}^3\text{-s}}\right\} = 71{,}691 \exp(-35{,}699/RT)\, P_{O_2} \quad (4)$$

where T is the particle temperature, K, and P_{O_2} is the oxygen partial pressure, kPa.

Comparison of this expression with char-O_2 data was, however, quite limited. Dutta, Wen and Belt (1975, 1977a) have presented results of C-CO_2 kinetic studies for a variety of coal chars. For Illinois #6 char the expression they present can be modified to give:

$$r = 1.1679\ 10^9\, d_p/T \exp(-59{,}260/RT)\, P_{CO_2} \quad (5)$$

where d_p is the particle diameter, m. Note that the unusual form of Eq. 5 is a result of forcing the rate expression into a shrinking core model form.

These rate expressions can be used to compute the combined reaction–diffusion rate for comparative purposes. The results expressed as the ratio of the combined rate to the diffusion-limited rate, are shown in Tables 1 and 2. As evident from Table 1, the char-O_2 reaction rate is diffusionally limited for large particles and kinetically limited for small particles. If the particle temperature exceeds the bulk temperature, Table 2, the diffusion limitations become more pronounced. For the char-CO_2 reaction, Table 1 indicates similar trends. In this case also, because of the exponential temperature dependence, the extent of particle superheat can be important. These conclusions are supported by the experimental findings of Sargeant and Smith (1973), Dutta et al. (1977b), and Chakraborty and Howard (1979). For polydispersed feeds limiting case reaction rate models may not be satisfactory. Therefore, for this study a single-film model with CO combustion in the interstitial gas and combined diffusion-reaction at the particle surface will be employed. It appears in fact that this choice of single-particle combustion model is the only valid one for AFBC conditions in general. Although the two-film model has been successfully used by Avedesian and Davidson (1973) to match their batch AFBC experiments, their reactor conditions (high O_2 concentrations) are atypical of normal AFBC operation.

TABLE 1. RATIO OF COMBINED RATE TO DIFFUSION-LIMITED RATE AT ATMOSPHERIC PRESSURE (CHAR TEMPERATURE = BULK TEMPERATURE)

Particle Size	Bulk Temp.	Char-O_2 Reaction[1] Reaction Rate Diff.-Limited Rate (O_2)	Char-CO_2 Reaction[2] Reaction Rate Diff.-Limited Rate (CO_2)
10μ	649°C	$3.326\ 10^{-5}$	0*
	871	$1.282\ 10^{-3}$	0
	1,093	$1.459\ 10^{-2}$	0
	1,315	$8.161\ 10^{-2}$	0
100	649	$3.325\ 10^{-4}$	0
	871	$1.266\ 10^{-2}$	0
	1,093	0.129	0
	1,315	0.456	$3.104\ 10^{-3}$
1,000	649	$3.326\ 10^{-3}$	0
	871	0.114	0
	1,093	0.597	$1.834\ 10^{-2}$
	1,315	0.894	0.238
10,000	649	$3.219\ 10^{-2}$	0
	871	0.562	$3.504\ 10^{-2}$
	1,093	0.937	0.651
	1,315	0.988	0.967

[1] 5% ambient oxygen.
[2] 10% ambient carbon dioxide.
* Less than 10^{-6}.

TABLE 2. EFFECT OF PARTICLE SUPERHEAT ON CHAR OXIDATION RATE FOR A 1,000-μm PARTICLE*

Bulk Temp.	Particle Temp.	Reaction Rate Diff.-Limited Rate
649°C	649°C	$3.329\ 10^{-3}$
	760	$2.551\ 10^{-2}$
	871	0.120
871	871	0.114
	982	0.333
	1,093	0.608
1,093	1,093	0.597
	1,204	0.794
	1,315	0.898

* Assumptions: 5% ambient oxygen, atmospheric pressure.

PREVIOUS FBC MODELS

A number of FBC models have been reported in the literature differing in the manner in which the solid phase is treated, in the single-particle combustion submodel that is used, as well as in the particular bubbling-bed reactor model that is selected. Since, as

TABLE 3. OPERATING CONDITIONS FOR FLUIDIZED-BED COMBUSTION CASE STUDIES

Pressure	Atmospheric
Bed Temp. (Nominal)	843°C (1,550°F)
Solid feed	
Type	Coal
Feed Rate	210.7 kg/h (464.5 lb/h)
Temperature	29.4°C (85°F)
Proximate Analysis	
Volatile Matter	34.3% (wt.)
Fixed Carbon	40.2
Ash	9.3
Moisture	16.2
Ultimate Analysis (daf)	
Carbon	81.6% (wt.)
Hydrogen	5.8
Oxygen	0.9
Sulfur	3.3
Nitrogen	8.4
Type	Limestone
Feed Rate	43.7 kg/h (96.4 lb/h)
Temperature	29.4°C (85°F)
Composition	
CaO (+MgO)	51.9% (wt.)
CO_2	40.9
H_2O	7.2
Gas Feed	
Feed Rate	260.6 kmol/h (574.5 lb mol/h)
Temperature	215°C (419°F)
Composition	
O_2	18.4% (mol)
N_2	76.8
H_2O	3.8
CO_2	1.0

will become apparent from our case studies, the last factor appears to be of secondary importance, we will review these models and pay particular attention to the first two-model components. From this point of view the models presented by Gibbs (1975) and Chen and Saxena (1977) are identical to that of Avedesian and Davidson. A distribution of particle sizes arises from a shrinking core solid reaction model, the bed is isothermal with particle temperatures equal to the emulsion-phase temperature, and the single-particle reaction rates are described by the two-film model over the entire range of particle sizes. Baron et al. (1977) assumed that the CO oxidation reaction occurs at the char surface rather than within the boundary layer. Horio and Wen (1975) and Rajan and Wen (1979) also assumed a shrinking core solid model. However, single-particle oxidation kinetics for the char-O_2 reaction were calculated from a single-film model with both kinetic and diffusional resistances included. CO oxidation occurred in the emulsion phase. The char-O_2 reaction was not considered. Gordon et al. (1976, 1978) modelled an oxygen-blown fluidized-bed combustor at three levels of sophistication. At the most detailed level a single-film reaction model including both diffusional and kinetic resistance for the char-O_2 and char-CO_2 reactions was used. Particle temperatures were computed as a function of residence time. All of these models assumed monosized solid feeds.

DEFINITION OF SIMULATED SYSTEM

In this study the reactor parameters selected were those corresponding to the Babcock and Wilcox (1978) experimental unit.

TABLE 4. REACTOR PERFORMANCE FOR BABCOCK AND WILCOX EXPERIMENTAL RUN 26 (BED ONLY)

Flue Gas Composition	
O_2	3.53% (mol)
CO	0.54
CO_2	12.56
Fixed Carbon Conversion	81.6
Oxygen Conversion	80.7

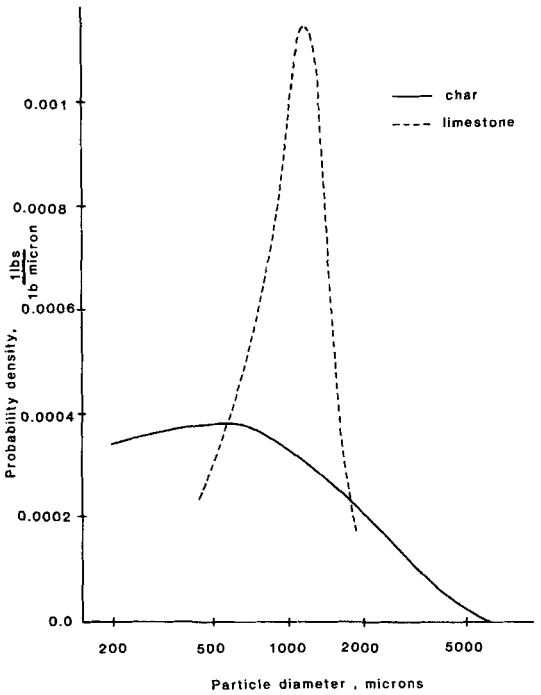

Figure 1. Probability density for fluidized-bed combustor feed.

That unit had a cross-sectional area of 0.93 m^2 (10 ft^2), expanded bed height of 0.42 m (1.37 ft) and no cyclones. The grid region consisted of 1,504 4-mm diameter orifices. Heat transfer internals consisted of a 0.91 m (3 ft) length of 0.0381 m (1½ in.) diameter schedule 40 pipe. The operating conditions and results of that run are reproduced in Tables 3 and 4. Note that the B&W reactor is fed coal and limestone. The former will undergo devolatilization and the latter will calcine. Both phenomena are known to occur very rapidly with time scales on the order of the solid mixing times in the bed (Beer, 1976). Thus, for this study, these phenomena are assumed to occur instantaneously and, consistent with the assumptions of CSTR interstitial gas and emulsion solids behavior, uniformly throughout the emulsion phase. The released volatile matter is assumed to immediately undergo the following set of combustion reactions:

$$2C + O_2 \rightarrow 2\,CO \qquad S + O_2 \rightarrow SO_2$$

$$4H + O_2 \rightarrow 2\,H_2O \quad \text{and} \quad 2O \rightarrow O_2$$

$$2N \rightarrow N_2 \qquad H_2O \rightarrow H_2O$$

The net effect of devolatilization is, thus, the same as that of an additional gaseous feed stream added solely to the emulsion phase. The resulting adjusted coal feed rate of 120.1 kg/h is that of the devolatilized coal (char). A similar adjustment is made for the limestone feed rate to result in an adjusted flow of 22.93 kg/h. It is assumed that neither devolatilization nor calcination altered the particle-size distributions of the coal or limestone feed streams respectively. Consequently, the densities of the feed char and limestone are also adjusted to 1,089 and 1,330 kg/m^3 respectively. The size distribution functions for the solid feeds which were graphically determined from the cumulative distributions given in Babcock and Wilcox (1978) are shown in Figure 1.

The Babcock and Wilcox unit has been simulated using the bed model described earlier (Overturf and Reklaitis, 1983). Since no internal cyclones or elutriated fines recycle were employed in the B&W unit, the freeboard region compartment has been deleted from consideration. The FBC model thus reduces to the compartments and flows shown in Fig. 2. The bed was assumed to contain two solids: the reacting char which is polydispersed in size and the nonreacting CaO which is treated as a monosized solid. The reaction of SO_2 with CaO is neglected because of the lack of reliable single-particle reaction kinetics. The char particles are assumed

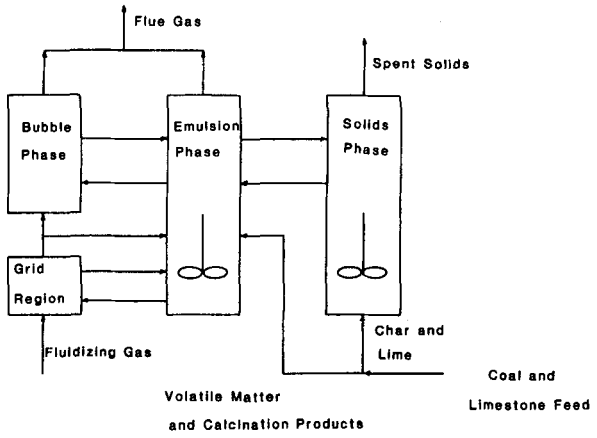

Figure 2. Schematic of fluidized-bed coal combustor model.

to react via reactions 1 and 2 with reaction rates computed according to Eq. 4 and 5 and the single-film model. The shrinking core reaction model is used including diffusion and reaction. Gas-phase CO oxidation, reaction 3, is assumed to occur in the grid, bubble-phase, and emulsion-phase compartments but not within the particle boundary layers. The rate of reaction 3 is predicted using the expression proposed by Howard et al. (1973).

$$r\left(\frac{\text{kmol } O_2 \text{ consumed}}{m^3 - s}\right) = 6.32 \times 10^7 \exp(-15{,}106/T) C_{CO} C_{O_2} C_{H_2O}^{1/2}$$

where the concentrations are in kmol/m^3. Note that the above rate expression includes a term reflecting the catalytic effect of water vapor.

The simulation is executed using the BED program (Overturf and Reklaitis, 1980) which incorporates the physical property and fluidization parameter prediction methods described in Part I. The BED program does, of course, generate a comprehensive report for each simulation. However, to compress the presentation we will give axial profiles and particle distribution curves in only a few cases. For the majority of the runs we will only report the following key output variables: the flue gas composition, the fixed carbon conversion, and the O_2 conversion. For complete output summaries, consult Overturf (1980) and Overturf and Reklaitis (1980).

CASE STUDIES

In this section we will present the results of a series of simulation case studies investigating the follow aspects of the FBC model.

- Influence of the grid region compartment as expressed in terms of the jet-to-emulsion transfer rates and average bubble size
- Sensitivity with respect to the bed void fraction
- Effect of emulsion gas temperature
- Influence of elutriation
- Sensitivity with respect to reaction rate constants
- Consequences of monosized vs. polydispersed feed
- Effect of particle superheat

While our first objective in presenting these case studies is to demonstrate that the model can predict experimentally observed results, a second and no less significant one is to identify the model parameters whose values are important in predicting the behavior of FBC reactors. In this manner we hope to be able to identify some of the weaknesses of previous modeling studies and to point out areas where further research would be best concentrated.

Grid Region Effects

The first question of concern is whether or not a separate model of the grid region is in fact necessary. In BED the grid region is modeled by treating the jets as plug-flow reactors through which all of the fluidizing gas must flow and which exchange heat and mass with the emulsion gas. In the absence of specialized correlations, the jet-to-emulsion transfer rates are related to the average bubble-to-emulsion transfer rates by a multiplicative factor, called the grid enhancement factor. Studies which evaluated the effect of this factor on predicted reactor performance are summarized in Table 5. The average bubble size computed for the actual bed conditions was used to compute the transfer coefficients for the remainder of the bed. The rate of jet-to-emulsion transfer, Table 5, affects the reactor performance up to a point beyond which further increase in the grid enhancement factor (>50) does not increase conversion.

TABLE 5. EFFECT OF GRID ENHANCEMENT FACTOR ON PREDICTED FLUIDIZED-BED COMBUSTOR PERFORMANCE

Grid Enhancement Factor	Flue Gas Composition % O_2	% CO	% CO_2	Fixed Carbon Conversion	Oxygen Conversion
10	9.23	0.49	7.19	21.8	47.4
25	5.69	0.42	10.76	61.0	67.6
50	4.41	0.32	12.10	75.0	74.9
75	4.18	0.28	12.33	77.0	76.2
100	4.07	0.26	12.43	77.6	76.8
150	3.93	0.25	12.55	77.6	77.6

Regardless of the value of the grid enhancement factor used, the predicted fixed carbon conversion is less than that observed experimentally for run 26 (81.6). The initial bubble size for the cases was 0.064 m and the average bubble size was 0.16 m. To determine the effect that the average bubble size had on the results a set of cases with a range of average bubble sizes was considered. Results for grid enhancement factors of 10 and 50 are shown in Table 6. For a large grid enhancement factor (50) nearly all of the incoming oxygen is transferred from the dilute to the emulsion phase within the grid region. Since little bubble-to-emulsion transfer occurs, reactor performance is insensitive to average bubble size. A typical set of dilute-phase oxygen concentration profiles is shown in Figure 3. Under these conditions reactor performance is limited by the reaction rates in the emulsion phase. An increase in bed height increases conversion only because of the increase in emulsion-phase volume.

On the other hand, for a grid enhancement factor of 10 a significant portion of the oxygen remains in the dilute phase, as can be seen from the axial profiles of oxygen concentration also shown in Figure 3. Thus, the amount of oxygen transferred from the bubbles to the emulsion phase, and thereby the reactor performance, does become sensitive to the average bubble size, Table 6. Reactor performance will, under these conditions, be more sensitive to bed height. It is furthermore interesting to note that, Figure 4, the initial bubble-to-emulsion mass transfer rates, which are related to $(1/d_B)^{3/2}$, are only a factor of 2 greater than the rates predicted

TABLE 6. EFFECT OF AVERAGE BUBBLE SIZE ON PREDICTED REACTOR PERFORMANCE

Avg. Bubble Size (m)	Flue Gas Composition % O_2	% CO	% CO_2	Fixed Carbon Conversion	Oxygen Conversion
Grid Enhancement Factor = 10					
0.030	4.06	0.25	12.45	77.26	76.9
0.061	4.27	0.32	12.24	76.74	75.7
0.122	6.82	0.46	9.61	48.39	61.1
0.160	9.23	0.49	7.19	21.80	47.4
0.183	10.20	0.54	6.19	11.49	41.9
Grid Enhancement Factor = 50					
0.030	2.92	0.24	13.22	74.5	83.3
0.061	3.80	0.25	12.64	77.15	78.4
0.122	4.17	0.28	12.34	77.17	76.3
0.160	4.41	0.32	12.10	75.0	74.9
0.183	4.62	0.35	11.87	72.8	73.7

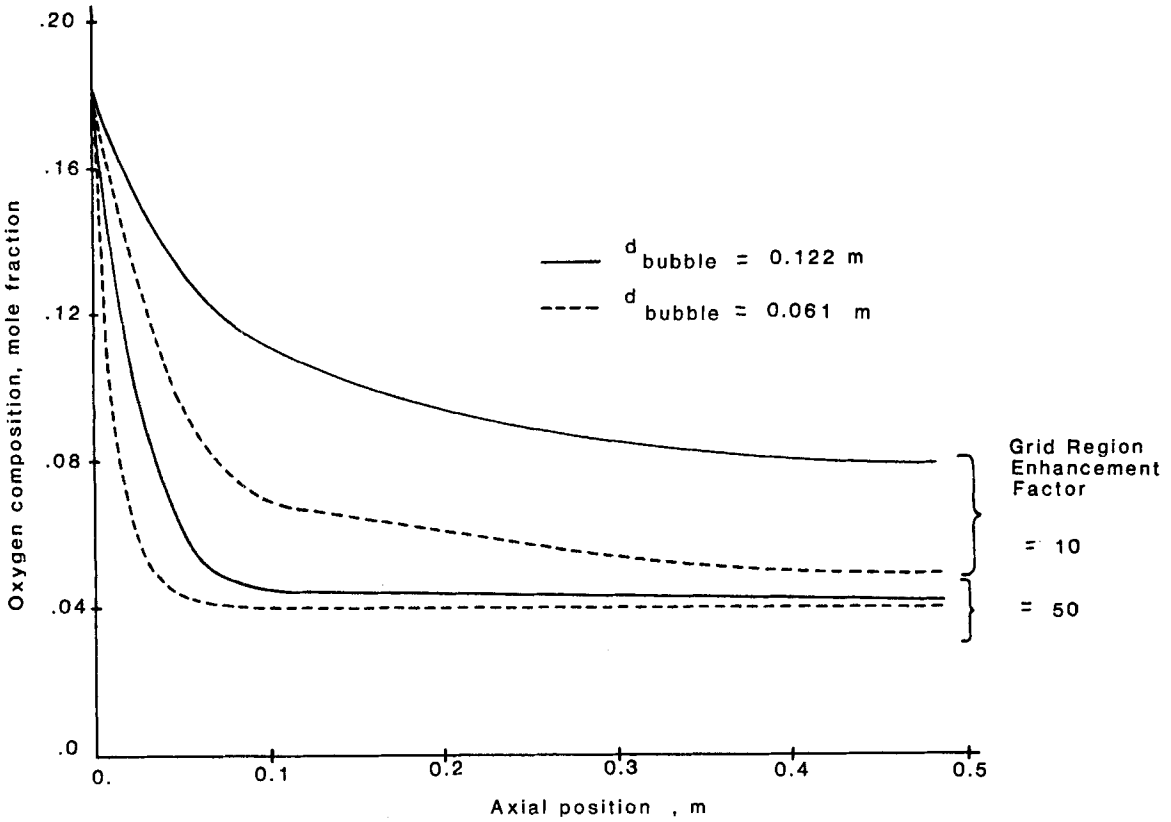

Figure 3. Dilute-phase oxygen composition profiles.

from the average bubble size. Thus the grid region phenomenon of rate enhancement by a factor of 50 reported by Behie and Kehoe (1973) cannot be explained in terms of bubble size alone as was implied by Rajan and Wen (1979).

These results suggest further that for reactor scale-up, in cases of high grid region activity, it is important to make certain that a similarity in grid region activity is maintained. The reactor height is not that critical. For cases of low grid region activity, performance will be sensitive to average bubble size and reactor height. Thus, the use of bed internals to control bubble size must be given careful attention. Similar conclusions can be drawn concerning the suitability of existing bubbling-bed models in representing reactor

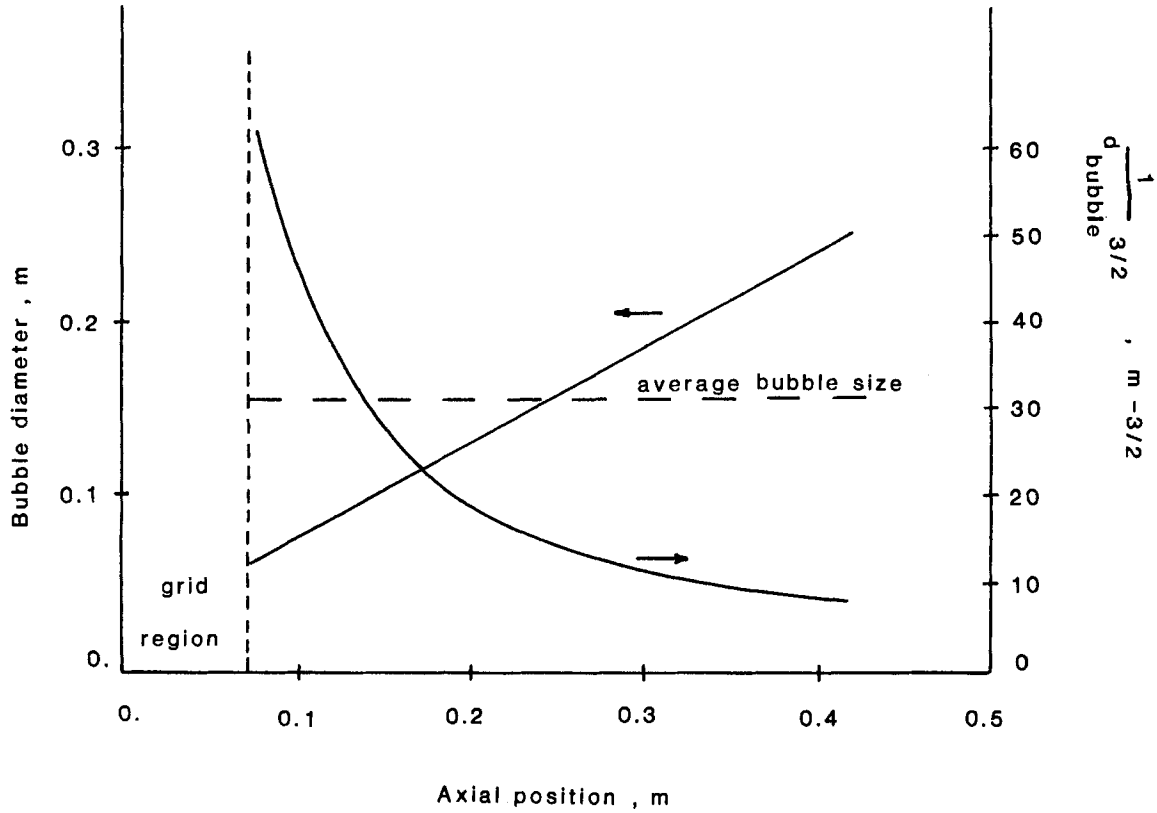

Figure 4. Bubble-size and bubble-to-emulsion transfer rates as functions of axial position.

TABLE 7. EFFECT OF EMULSION-PHASE TEMPERATURE ON FLUIDIZED-BED COMBUSTOR PERFORMANCE

Emulsion Phase Temp. °C	Flue Gas Composition % O_2	% CO	% CO_2	Fixed Carbon Conversion	Oxygen Conversion
982	6.27	0.61	10.07	55.2	64.3
1,038	5.00	0.47	11.42	68.8	71.5
1,093	4.41	0.32	12.10	75.0	74.9
1,148	4.06	0.21	12.50	78.8	76.9
1,204	3.80	0.14	12.80	81.9	78.4

behavior. Certainly, if most interphase transfer occurs within the grid region, the typical bubbling-bed model is of questionable benefit. In fact, the bed could well be simply modeled as a CSTR or, perhaps, totally ignored, while the grid region should be the primary emphasis. On the other hand, if reactor performance is determined by the transfer of reactant from the bubbles to the emulsion phase, bubbling-bed models should prove useful.

In all cases, the importance of the grid region can only be determined from experimental results. Thus, the allocation of experiments to identify the role of the grid region should be a primary concern in fluidized-bed reactor studies. In the case of the B & W runs, it is clear that to achieve a level of conversion similar to run 26, a grid region model must be included. A grid enhancement factor of 50 was selected for use in the remainder of the parameter studies as a reasonable compromise based in part on the Behie and Kehoe (1973) recommendations and on the results shown in Table 5.

Void Fraction

It is well known that predictions of the void fraction at minimum fluidization, ϵ_{mf}, for polydispersed feed using available correlations are generally of low reliability (IGT, 1978). The appropriate value of this parameter must be established experimentally. For this study a typical value of 0.5 was used in the absence of experimental data. In proceeding from an ϵ_{mf} value of 0.4 to one of 0.6 the flue-gas composition changes from 4.37, 0.38, and 12.1% to 4.49, 0.28, and 12.04% for O_2, CO, and CO_2, respectively. The fixed carbon conversion changes from 75.8 to 73.7 and the oxygen conversion from 75.1 to 74.5. The dilute-phase gas composition profiles for the base case ($\epsilon_{mf} = 0.5$), Figure 5, indicate that overall reactor conversion is limited by emulsion-phase conversion which is itself limited by the perfect mixing assumption for the emulsion phase. Clearly, the reaction in the dilute phase nears completion. Decreasing ϵ_{mf} decreases the volume of gas emulsion phase and thus the oxygen residence time. However, for fixed bed volume, decreasing ϵ_{mf} also increases the amount of solid in the bed and hence its residence time. These two effects offset each other making the net change in emulsion-phase behavior difficult to predict. Since approximately 10% ot the total gas flow passes through the emulsion phase, the effect of ϵ_{mf} on the overall bed performance is small.

Emulsion-Phase Temperature

The temperature of the emulsion gas phase is another potentially

TABLE 8. EFFECT OF EMULSION-PHASE TEMPERATURE ON CO CONVERSION

Emulsion Phase Temp. °C	Emulsion Phase $\frac{CO_2}{(CO + CO_2)}$ mol %	Flue Gas $\frac{CO_2}{(CO + CO_2)}$ mol %
982	0.614	0.943
1,038	0.726	0.96
1,093	0.813	0.974
1,148	0.873	0.983
1,204	0.913	0.989
Experimental		0.959

TABLE 9a. EFFECT OF PARTICLE ELUTRIATION ON FLUIDIZED-BED COMBUSTOR PERFORMANCE

	Flue Gas Composition % O_2	% CO	% CO_2	Fixed Carbon Conversion	Oxygen Conversion
Elutriation Included	4.41	0.32	12.10	75.0	74.9
Elutriation Neglected	3.34	0.39	13.12	91.1	81.0
Experimental	3.53	0.54	12.56	81.6	80.7

significant model parameter. For simulation, it was assumed that the experimentally measured temperature (838°C) was that of the emulsion gas phase, which was controlled by the removal of heat through immersed surfaces. The base case dilute-phase temperature profile, Figure 5, is not significantly different from the emulsion-phase temperature since most of the exothermic homogeneous reaction occurs within the emulsion phase. The solids temperatures are also not significantly higher (discussed later), so that for this example any question of which temperature the thermocouple really measures is immaterial. It is certain, however, that thermal gradients do occur around cooling surfaces and that both thermal and concentration gradients occur in the vicinity of the solid and gas feed ports. These local gradients can alter emulsion-phase conversion. As shown in Table 7, an increase in the emulsion-phase temperature increases both the solid conversion and the extent of CO oxidation. However, while CO conversion in the emulsion phase increases, Table 8, the overall effect on the CO_2 fraction is small. Thus, we can conclude that the temperature has a significant influence on the fixed carbon conversion but only a modest impact on the CO_2 concentration.

Elutriation Rates

In all of the preceding cases, bed elutriation rates were computed from the correlation of Merrick and Highley (1974). In the Babcock and Wilcox work, elutriated fines were collected but not recycled to the bed. The effect that ignoring the elutriation of solid particles has on predicted reactor performance is shown in Tables 9a and 9b. When elutriation is not allowed, the increased char residence time results in higher levels of conversion. As pointed out by Rajan and Wen (1979), the Merrick and Highley correlation should be used in its original form only when the freeboard height in question is the same as that used by Merrick and Highley in their studies. For shorter freeboard heights, as is the case here, the elutriation rate will exceed the rate predicted by the correlation. However, the Babcock and Wilcox pilot plant has heat transfer tubes in and immediately above the upper part of the bed which should hinder elutriate flow. Nonetheless, the predicted elutriation rate of 8.39 g/s, is lower than the experimental results, 14.1 g/s. However, the bed char content is, Table 9b, higher than the experimental value in both the elutriation and the no-elutriation cases. This anomalous behavior will be reconsidered in later discussion. The significant point to retain for the present is that elutriation does have a significant effect on the fixed carbon and oxygen conversions as well as on the bed char fraction.

TABLE 9b. STEADY-STATE COMBUSTOR-BED COMPOSITIONS

	Experimental wt. %	Predicted Base Case wt. %	Predicted No Elutriation wt. %
CaO	64.5		
SO_3	25.2		
CO_2	0.4		
Total Sorbent	90.1	82.8	60.3
C	0.2		
Inert	9.7		
Total Char	9.9	17.2	39.7

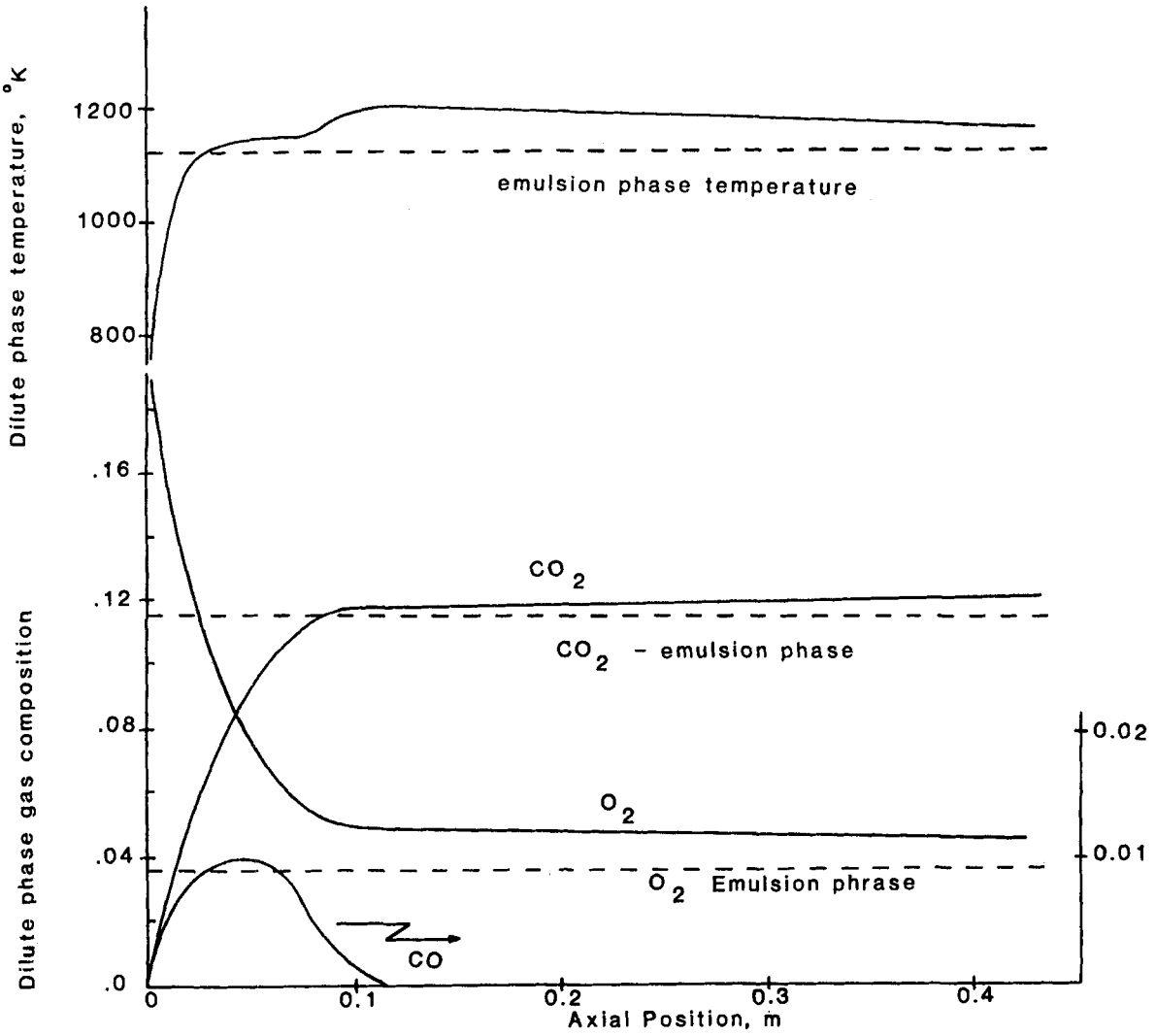

Figure 5. Dilute-phase composition and temperature profiles.

Reaction Rates

A further important set of model parameters are the kinetic and diffusion rates which govern the heterogeneous and homogeneous reactions. Clearly at these higher temperatures the heterogeneous reaction rates are influenced by diffusional effects. In the model, the Sherwood and Nusselt numbers were assumed to be equal to 2.0; they could well assume somewhat different values. Moreover, Field's kinetic data were based primarily on experiments with carbon. The char-O_2 reactivity may be significantly different from that of carbon. To investigate the effects of variations in diffusion rate on predicted reactor behavior the runs shown in Table 10 were carried out. Note that a decrease in the diffusion rate substantially affects flue-gas composition and fixed carbon conversion. An increase has relatively little influence indicating that the kinetic rate becomes limiting.

TABLE 10. EFFECT OF DIFFUSION RATE ON REACTOR PERFORMANCE: BOTH HETEROGENEOUS REACTIONS

Rate Multiplier	Flue Gas Composition % O_2	% CO	% CO_2	Fixed Carbon Conversion	Oxygen Conversion
0.01	7.93	0.221	8.63	31.9	56.9
0.1	5.25	0.278	11.28	66.0	71.4
0.5	4.63	0.309	11.88	72.5	74.8
2.0	4.51	0.316	12.00	73.8	75.5
10.0	4.47	0.318	12.03	74.1	75.7
100.0	4.46	0.318	12.04	74.2	75.7

A similar series of runs was carried out to investigate the effects of variation in the rate of the CO oxidation reaction. As shown in Table 11 for the no elutriation case, the CO composition is quite sensitive to the relative rate of oxidation. As might be expected, with reduced O_2 consumption by CO oxidation, the carbon conversion increases because of the increased O_2 availability. Recall that the rate expression for CO oxidation includes the partial pressure of water. In our runs the water concentration was assumed to be constant at its level in the inlet stream. Since the CO level predicted by the simulation is too low, it may be appropriate to add the char-steam reaction to the model. Any char-steam reaction would decrease the amount of water vapor in the emulsion phase and, thus, result in a reduced CO oxidation rate.

Finally, a series of runs was carried out to deduce the relative contribution of the char-CO_2 reaction. The results, not tabulated here, indicated that for the conditions of the present case study, the reactor performance was virtually identical to the base case.

TABLE 11. EFFECT OF HOMOGENEOUS REACTION RATE ON REACTOR PERFORMANCE: NO ELUTRIATION

Rate Multiplier	Flue Gas Composition % O_2	% CO	% CO_2	Fixed Carbon Conversion	Oxygen Conversion
0.67	3.30	0.495	13.11	92.7	82.1
0.50	3.27	0.577	13.09	93.5	82.2
0.25	3.23	0.790	13.00	95.2	82.4
0.10	3.24	1.054	12.84	96.5	82.4

TABLE 12. SINGLE-PARTICLE CHARACTERISTICS FOR BASE-CASE FLUIDIZED-BED COMBUSTOR DESIGN

Particle Size (m)	Particle Temp. K	Heterogeneous Reaction Rates (kmol/m²s) $2C + O_2 \rightarrow 2CO$	$C + CO_2 \rightarrow 2CO$	Elutriation Constant kg/kg
$1.37\ 10^{-4}$	1,116	$1.45\ 10^{-5}$	$1.52\ 10^{-7}$	$1.73\ 10^{-1}$
$6.98\ 10^{-4}$	1,123	1.52	1.81	$5.00\ 10^{-5}$
$1.62\ 10^{-3}$	1,126	1.45	1.94	$7.93\ 10^{-11}$
$2.76\ 10^{-3}$	1,126.6	1.33	1.96	$5.25\ 10^{-18}$
$3.93\ 10^{-3}$	1,126	1.22	1.95	$1.79\ 10^{-25}$
$5.00\ 10^{-3}$	1,126	1.13	1.94	$4.34\ 10^{-32}$
$5.49\ 10^{-3}$	1,125.6	1.07	1.92	$7.58\ 10^{-37}$
$6.10\ 10^{-3}$	1,125.6	1.05	1.92	$5.25\ 10^{-39}$

The effect of using the two-film kinetic model could not be investigated using the present fluidized-bed model because it was not possible to satisfy the single-particle enthalpy balances with the O_2 compositions of this study.

MONOSIZED VS. POLYDISPERSED FEED

Having compared the sensitivity of the FBC performance to variations in some of the key model parameters, we now consider the effect of a simplification often made in fluidized-bed combustor modeling: use of a monosized coal feed distribution. For a monosized feed comprised of 1,150μ particles, a flue-gas composition of 3.44, 0.38, and 13.02% O_2, CO, and CO_2, respectively, is obtained; a carbon conversion of 91.3%; and an oxygen conversion of 74.9%. Recall that the corresponding results for the polydispersed base case are 4.41, 0.32, and 12.1 for the compositions and 75.0 and 74.9 for the conversions. Representing the coal feed as monosized particles of average particle size thus produces a difference in performance which is large in comparison to the effect of many of the factors already discussed. An examination of the single-particle characteristics; reaction rates and elutriation constants, Table 12, reveals that the disparity is almost certainly due to the difference in fluidization properties rather than in reaction rates. Notice that the results for the monodispersed feed are quite similar to the results shown in Table 9a for no solid elutriation.

Particle Superheat

Another assumption often used in FBC modeling is that the particle temperatures are the same as the emulsion gas temperature. Table 12 indicates that the largest degree of particle superheat is on the order of 16°C, certainly a modest temperature difference. A run was made to determine the effect of no superheat and the results were compositions of 4.51, 0.32, 12.0 and conversions of 73.4 and 74.3. As expected the overall difference from the base case is modest; however, the difference in the fixed carbon conversion suggests that large conversion differences could be observed if the superheat were higher. One parameter influencing particle superheat is the char emissivity. Accordingly a series of runs were carried out in which the emissivity was decreased from its base case value by multiplicative factors, Table 13.

TABLE 13. EFFECT OF CHAR EMISSIVITY ON PREDICTED REACTOR PERFORMANCE

Emissivity Factor	Flue Gas Composition % O_2	% CO	% CO_2	Fixed Carbon Conversion	Oxygen Conversion
1.0	4.41	0.32	12.10	74.9	75.0
0.5	4.52	0.315	11.99	73.5	75.4
0.1	4.42	0.32	12.08	74.0	75.9
0.01	4.14	0.34	12.35	74.6	77.5

TABLE 14. SINGLE-PARTICLE CHARACTERISTICS FOR A LOW CHAR EMISSIVITY FACTOR OF 0.01

Particle diameter (m)	Particle Temp. (K)	Heterogeneous Reaction Rates (kmol/m²s) $2C + O_2 \rightarrow 2CO$	$C + CO_2 \rightarrow 2CO$
$1.37\ 10^{-4}$	1,115	$1.45\ 10^{-5}$	$1.51\ 10^{-7}$
$6.98\ 10^{-4}$	1,134	1.63	2.38
$1.62\ 10^{-3}$	1,193	2.74	8.79
$2.76\ 10^{-3}$	1,275	3.72	$4.25\ 10^{-6}$
$3.93\ 10^{-3}$	1,289	3.11	5.42
$5.00\ 10^{-3}$	1,291	2.65	5.52
$5.49\ 10^{-3}$	1,291	2.42	5.42
$6.1\ 10^{-3}$	1,291	2.37	5.37

Note that the fixed carbon conversion exhibits a minimum because of competing effects. Single-particle characteristics for an emissivity factor of 0.01 shown in Table 14 reveal that the temperatures of the larger particles have increased when compared to the results for the base case, Table 12. Moreover, the char oxidation rates for the larger particles have increased accordingly. Note, however, that the increased rate of the char-CO_2 reaction has limited the temperature rise of the particles. Even though the single-particle reaction rates have increased, predicted fixed carbon conversions remain lower than observed experimentally. It is noteworthy that the char level in the bed was reduced to 12.5%, closer to the measured 9.9% than the base case value of 17.2%. Yet, the char elutriation rates are still low, 11.8 g/s vs. 14.1 g/s.

NUMERICAL ACCURACY

Two key factors influencing the accuracy of the model predictions are the number of quadrature points used to evaluate the dilute- and jet-phase average concentrations and temperatures and the number of collocation points used to represent the solution of the particle balance equation. For all of the cases presented in this study, ten quadrature points were used to represent the dilute-phase and grid-region profiles. A check of how well the quadrature formula represents the actual integration can be determined by comparing the dilute-to-emulsion-phase mass flux based on the dilute-phase balances to the flux used in the emulsion-phase balances. The flux for the emulsion-phase balances is computed from the quadrature formula. If the two values do not agree, more quadrature points are required. A similar check can be performed for the grid region.

Unfortunately there is no similar simple check on the accuracy of the solids distribution representation. A direct check against the experimentally determined bed distribution is not useful, Figure 6, because the bed distribution is dominated by the limestone distribution. Thus even though there is a substantial difference in the char-size distribution, this difference is submerged in the combined distribution reported. An indirect check of numerical accuracy can in principle be obtained by simply repeating the simulation with different number of collocation points. Using this check is difficult because, to represent the empirical feed-size distribution, that distribution was represented in terms of an interpolating polynomial numerically fitted at the collocation points. Thus, as the number of collocation points is increased, the solid-feed distribution accuracy and the solution accuracy change. Scatter in the solid-feed distributions makes it difficult to ascertain whether differences in the results are due to a better representation of the solids in the bed or a more or less accurate description of the solid feed. Use of a monosized feed eliminates fluctuation in the feed specification. Consequently, for determining the suitable number of collocation points, test runs were made with the monosized-feed approximation. Based on these tests seven interior points were found sufficient to approximate the char distribution for each of the coordinates for the combustion case studies. As noted earlier the limestone was treated as a monosized solid.

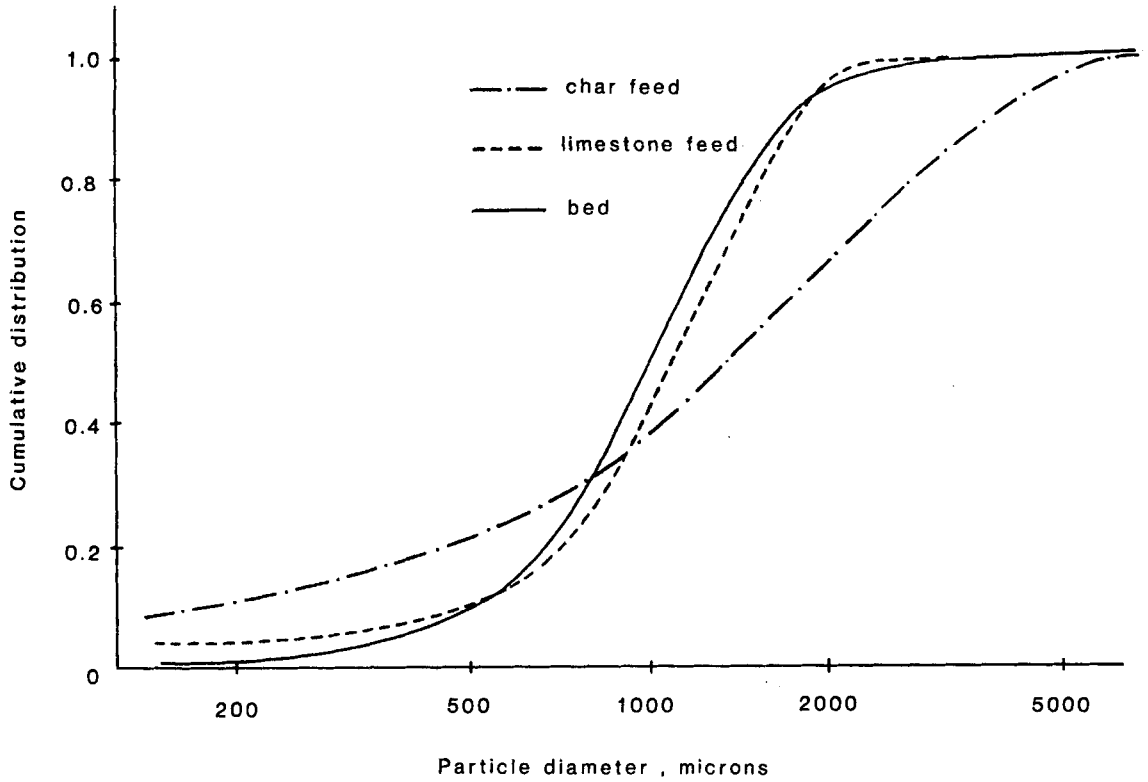

Figure 6. Fluidized-bed combustor particle-size distributions (measured).

DISCUSSION

The case studies assembled earlier indicate the range of performance predictions possible by judicious selection of model parameter values. As shown in Table 14, the predicted CO concentration for the base case (elutriation included) is too low. This is due to the low fixed carbon conversion which results in a high emulsion-phase oxygen content and, therefore, favors homogenous CO oxidation to CO_2. The total amount of carbon in the flue gas is 12.42 mol carbon/mol flue gas vs. 13.10 mol carbon/mol flue gas observed experimentally. If elutriation is neglected, the predicted fixed carbon conversion exceeds the observed value since the more reactive smaller particles are allowed to remain in the bed. Nevertheless, the CO content in the flue gas is still too low. However, a modest decrease in the rate of the homogeneous reaction can readily account for this. Thus, it is obvious that a suitable adjustment of the elutriation rates, a reduction in the CO oxidation rate, and a decrease in the heterogeneous overall rates will lead to as close a match of the experimental performance as desired. However, the bed char to sorbent ratio remains problematic. One possible clue is offered by the fact that the experimental C to inert (ash) ratio in the bed is substantially lower than the fixed carbon to ash ratio in the feed coal. For strictly shrinking core solid behavior with the instantaneous attrition of ash, the carbon/inert ratio would remain constant. This indicates that a continuous reaction model may be more appropriate for at least a portion of the reactive particles. If this is the case, the char densities, elutriation and fluidization characteristics will all be affected, ultimately influencing both the elutriation rate and the bed carbon content.

ACKNOWLEDGMENT

This work was supported under U.S. DOE Contracts EX-76-C-01-2275 and DE-AC21-79MC 11633 with Purdue University.

LITERATURE CITED

Avedesian, M. M., and J. F. Davidson, "Combustion of Carbon Particles in a Fluidized Bed," *Trans. Instn. Chem. Engrs.*, **51**, 121 (1973).

Babcock and Wilcox Co, "Summary Evaluation of Atmospheric Pressure Fluidized Bed Combustion Applied to Electric Utility Large Steam Generators," EPRI FP-308, Project 412-1, Final Report (Oct., 1976).

Babcock and Wilcox Co., "SO_2 Absorption in Fluidized Bed Combustion of Coal—Effect of Limestone Particle Size," EPRI FP-667, Project 719-1, Final Report (Jan. 1978).

Baron, R. E., J. L. Hodges, and A. F. Sarofin, "Mathematical Model for Predicting Efficiency of Fluidized Bed Steam Generators," AIChE Annual Meeting, Paper No. 80a, New York (1977).

Beer, J. M. "The Fluidized Combustion of Coal," 16th Symp. (Int.) on Combustion, The Combustion Inst. (1976).

Behie, L. A., and P. Kehoe, "The Grid Region in a Fluidized Bed Reactor," *AIChE J.*, **19**, 5, 1070 (1973).

Caram, H. S., and N. R. Amundson, "Diffusion and Reaction in a Stagnant Boundary Layer about a Carbon Particle," *Ind. Eng. Chem. Fund.*, **16**, 171 (1977).

Chakraborty, R. K., and J. R. Howard, "Carbon Combustion Rates and Temperatures in Shallow Fluidized Beds," AIChE 86th Nat. Meeting, Paper No. 57d, Houston (1979).

Chen, T. P., and S. Saxena, "Mathematical Modelling of Coal Combustion in Fluidized Beds with Sulfur Emulsion Control by Limestone or Dolomite," *Fuel*, **56**, 401 (1977).

Dutta, S., C. Y. Wen, and J. Belt, "Reactivity of Coal and Char in CO_2 Atmosphere," Preprints—Div. of Full Chemistry, Amer. Chem. Soc., **20** (3), 103 (1975).

Dutta, S., C. Y. Wen, and R. J. Belt, "Reactivity of Coal and Char. 1. In Carbon Dioxide Atmosphere," *Ind. Eng. Chem.*, Process Des. Dev., **16**, No. 1, 30 (1977a).

Dutta, S., C. Y. Wen, and R. J. Belt, "Reactivity of Coal and Char 2, in Oxygen-Nitrogen Atmospheres," *Ind. Eng. Chem.*, Process Des. Dev., **16**, No. 1, 31 (1977b).

Field, M. A., D. W. Gill, B. B. Morgan, and P. B. W. Hauksley, *Combustion of Pulverized Coal*, BCURA, Leatherhead (1967).

Gibbs, B. M., "A Mechanistic Model for Predicting the Performance of a Fluidized Bed Coal Combustor," *Inst. of Fuel Symp. Ser.*, No. 1 (1975).

Gordon, A. L., and N. R. Amundson, "Modelling of Fluidized Bed Reactors-IV Combustion of Carbon Particles," *Chem. Eng. Sci.*, **31**, 1163 (1976).

Gordon, A. L., H. S. Caram, and N. R. Amundson, "Modelling of Fluidized Bed Reactors-V, Combustion of Carbon Particles—An Extension," *Chem. Eng. Sci.*, **33**, 713 (1978).

Horio, M., and C. Y. Wen, "Analysis of Fluidized Bed Combustion of Coal with Limestone Injection," *Fluidization Technology*, **II**, Proceedings of the Int. Fluidization Conf., Pacific Grove, CA (1975).

Horio, M., and C. Y. Wen, "Simulation of Fluidized Bed Combustors," AIChE Annual Meeting, Paper No. 48f, Chicago (1976).
Hougen, O. A., K. M. Watson, and R. A. Ragatz, *Chemical Process Principles*, 2nd Ed., Wiley, NY (1954).
Howard, J. B., G. C. Williams, and D. B. Fine, 14th Symp (Int.) on Combustion, The Combustion Institute, Pittsburgh, 975 (1973).
Inst. of Gas Tech., *Coal Conversion Systems Technical Data Book*, Prepared for the Department of Energy, Chicago, (1978).
Merrick, D., and J. Highley, "Particle Size Reduction and Elutriation in a Fluidized Bed Process," *AIChE Symp. Ser.*, No. 137, **70**, 366 (1974).
Mon, E., and N. R. Amundson, "Diffusion and Reaction in a Stagnant Boundary Layer about a Carbon Particle. 2. An Extension," *Ind. Eng. Chem. Fund.*, **17**, No. 4, 313 (1978).
Mon, E., and N. R. Amundson, "Diffusion and Reaction in a Stagnant Boundary Layer about a Carbon Particle 3. Stability," *Ind. Eng. Chem. Fund.*, **18**, No. 2, 162 (1979).
Overturf, B. W., and G. V. Reklaitis, "Bed: A Generalized Model of a Fluidized Bed Gas-Solid Reactor," Purdue Research Foundation, W. Lafayette, IN (1980).
Overturf, B. W., and G. V. Reklaitis, "A Fluidized Bed Reactor Model with Generalized Particle Balances: Part I: Formulation and Solution," *AIChE J.*, **29** (Sept. 1983).
Overturf, B. W., "Toward a Generalized Description of Gas-Solid Reaction in a Fluidized Bed Reactor," PhD Thesis, Purdue University, W. Lafayette, IN (1980).
Rajan, R., and C. Y. Wen, "Fluidized Bed Coal Combustor Modeling," AIChE Nat. Meeting, Paper No. 57a, Houston (1979).
Sergeant, G. D., and I. W. Smith, "Combustion Rate of Bituminous Coal Char in the Temperature Range 800 to 1700 K," *Fuel*, **52**, 52 (1973).

Manuscript received October 6, 1981; revision received October 5, and accepted October 20, 1982.

Anomalous Diffusion of Vapors through Solid Polymers

Part I: Irreversible Thermodynamics of Diffusion and Solution Processes

P. NEOGI

Department of Chemical Engineering
University of Missouri-Rolla
Rolla, MO 65401

The solubility and diffusivity of vapors in polymers below and in the vicinity of glass transition temperature are known to be explicitly time-dependent. It is assumed here that the polymers are in nonequilibrium states, characterized by an internal order. The latter relaxes with time and moves towards equilibrium. The changes in the internal order bring about changes in the properties of the polymer-solute system.

The time dependence of diffusivity and solubility has been derived for isothermal processes not far from equilibrium. Well-known procedures for analyzing relaxing systems are used to obtain the above results, and the knowledge of how the internal order is related to the molecular properties is not required.

SCOPE

The anomalous effects that are observed in the penetration of a vapor into solid polymers near and below the glass transition temperatures are well known and are caused by the relaxation in the polymer. As a result of these changes, the diffusivity and the solubility change with time. As a first step towards quantifying these effects, it is necessary to obtain the above as functions of time. These have been obtained here using the well-known ideas from irreversible thermodynamics. Using these forms, the mass transfer rates to such systems can be determined; a systematic study of diverse anomalies known from the experiments can be undertaken.

CONCLUSIONS AND SIGNIFICANCE

The time dependence of diffusion and solubility of a vapor penetrating into a solid polymer below or near the glass transition temperature has been obtained. Such media see molecular relaxation in time, and the above time effects are due to this relaxation and proceed at the same rate. The analysis has the advantage that a molecular model for the relaxation is not necessary to arrive at the results. However, it also proves to be a shortcoming since it is not possible to relate the above effects to the glass transition temperature. Use of molecular or phenomenological theories can be incorporated to introduce this feature. The generality of the present analysis allows the incorporation of such theories. However, the results are sufficient to analyze and unify many of the diverse anomalous effects observed in the sorption experiments on such systems and undertaken in Part II.